

# Is Dielectrophoretic Movement through Micro Channel with Asymmetric Surface Electrodes Fabricated by Photolithography Technique Effective to Sort Flowing Cell?

Shigehiro Hashimoto, *Member IEEE*  
dept. Mechanical Engineering  
Kogakuin University  
Tokyo, Japan  
shashimoto@cc.kogakuin.ac.jp

Kiyoshi Yoshinaka  
Health and Medical Research Institute  
National Institute of Advanced Industrial Science & Technology  
Tsukuba, Japan  
k.yoshinaka@aist.go.jp

**Abstract**— A flow channel with surface electrode has been designed to detect dielectrophoretic movement of floating myoblast. In the micro flow-channel, a pair of asymmetric surface electrodes of titanium coating (thickness of 200 nm) were fabricated by photolithography technique: the triangular electrode with the tip angle of 0.35 rad, and the rectangular electrode of the flat edge as the reference. The cyclic alternating square wave of the electric current was applied between the electrodes. The suspension of C2C12 (mouse myoblast cell line) was injected into the channel, and the shifted movement of each flowing cell was measured at the microscopic movie image. Experimental results of the pilot test show that the absolute value of the amplitude of the acceleration by the electric field, which is perpendicular to the flow direction, increases with the radius of each cell. The shifted movement of 70  $\mu\text{m}$  is realized at the adjusted electric parameters: the frequency of 3 MHz, and the amplitude of electric current of  $\pm 7.5$  mA.

**Keywords**— *biomedical engineering, cell sorting, dielectrophoresis, surface electrode, C2C12, photolithography*

## I. INTRODUCTION

The movement of a biological cell suspended in a medium is governed by several factors: movement of the medium, gravity [1], electric force, Van der Waals force, and affinity of the surface. In a lot of studies, various methods have been applied to control the movement of cells *in vitro*: the flow [2], the shear field [3], the filter, the slit [4–6], the magnetic field [7], the gravitational field [8], the laser [9], and the electric field [10]. These methods might contribute to several applications of the manipulation of cells [11]: detection of targeted cells [12], sorting of cells [13], arrangement of cells to make a tissue, and measurement of the character of cells [14].

Movement of a charged particle depends on the electric field. The effect is applied to the electrophoresis device [15]. When a particle is subjected to a non-uniform electric field, the force acts even on the non-charged particle, because the polarization generates in the particle. The phenomenon is called dielectrophoresis [16]. The force of dielectrophoresis depends on the several parameters: the electrical property of the particle, the shape and the size of the particle [17], the electrical property of the medium, and the electric field (the amplitude and the frequency).

Electrophoresis is a phenomenon, in which a particle is moved by the Coulomb force between the charge of the particle and the electric field. Dielectrophoresis [18], on the

other hand, is a phenomenon, in which a particle moves due to the interaction between the electric field and the charge induced in the neutral particle, when the particle is placed in a non-uniform electric field. With the aid of the micromachining technique [19], many kinds of micro systems were designed. In some systems, dielectrophoresis was applied to sort biological cells floating in the medium.

In the present study, a flow channel with asymmetric surface electrodes has been designed using the photolithography technique to sort cells by the dielectrophoretic movement. After optimizing the electric parameters, the shifted movement has been analyzed in relation to the radius of each floating cell *in vitro*.

## II. METHODS

### A. Design of Surface Electrode

To incorporate electrodes with the designed figure in the micro flow-channel, the titanium film coating was used for the surface electrode. The thickness of coating is 200 nm on the glass plate. After several trials for optimization, the design of the electrodes were decided as follows. One of the surface electrodes has a triangle shape with the tip angle of 0.35 rad. The other reference electrode has a flat edge (Fig. 1). The shortest connecting line between electrodes is vertical to the flow direction: 0.1 mm distance.

### B. Deposition of Titanium

The surface of the glass plate was hydrophilized by the oxygen plasma ashing by the reactive ion etching system, before the deposition of titanium. Titanium was deposited on the surface of the glass plate in the electron beam vapor deposition apparatus (Fig. 2). After a lot of trials, the protocol of fabrication of the surface electrodes incorporated micro flow-channel was made as follows.

### C. Photomask A for Triangle Tip of Electrode

The positive photoresist material of OFPR-800LB was coated on the titanium with the spin coater. The photoresist was baked at the hotplate at 338 K for one minute and at 368 K for three minutes, successively.

The pattern of the electrode with the flow channel was drawn on the photomask with a laser drawing system. The photoresist was developed with tetra-methyl-ammonium hydroxide for two minutes, rinsed with the distilled water, and dried.

The titanium coated plate was etched with the plasma gas using RIE-10NR. For etching, the gas of SF<sub>6</sub> with Ar was applied at 75 W at 4 Pa for seven minutes.

#### D. Photomask B for Electrode

The titanium coated glass plate was hydrophilized by the oxygen plasma ashing by the reactive ion etching system. The negative photoresist material of low viscosity (SU-8) was coated on the titanium with the spin coater. The photoresist was baked at the hotplate at 338 K for one minute and at 368 K for three minutes, successively.

The photomask A was mounted on the surface of SU-8, and the photoresist was exposed to the UV (ultraviolet) light through the photomask in the mask aligner. The photoresist was baked at the hotplate at 338 K for one minute and at 368 K for three minutes, successively. The photoresist was developed with SU-8 Developer. The glass surface with the micro pattern was rinsed with IPA (2-propanol) for one minute, and with the pure water for one minute. After drying, the plate was etched with the plasma gas using RIE-10NR. For etching, the gas of SF<sub>6</sub> with Ar was applied at 75 W at 4 Pa for seven minutes. The areas at the bands of both ends were covered with the polyimide tapes (to protect the photoresist material from the UV light) to leave the part of titanium coating for extended electrodes.

#### E. Photolithography process for surface electrodes

The titanium coated glass plate was hydrophilized by the oxygen plasma ashing for five minutes at 100 W by the reactive ion etching system. The positive photoresist material of OFPR-800LB was coated on the titanium with the spin coater. The photoresist was baked at the hotplate. The photomask B was mounted on the surface of SU-8, and the photoresist was exposed to the UV light through the mask in the mask aligner. The photoresist was developed with tetramethyl-ammonium hydroxide (NMD-3) for two minutes, rinsed with the distilled water. After drying, the plate was etched with the plasma gas using RIE-10NR. For etching, the gas of SF<sub>6</sub> with Ar was applied at 75 W at 4 Pa for seven minutes.

#### F. Lower Plate of Flow Channel

To make the groove of the flow channel (width of 0.5 mm, length of 18 mm, and depth of 0.04 mm), the photomask C was made by the same process as the photomask A. The surface of the electrodes was hydrophilized by the oxygen plasma ashing by the reactive ion etching system. The negative photoresist material of low viscosity (SU-8) was coated on the surface electrodes with the spin coater. The coating condition was adjusted to make the layer of thickness (correspond to the height of the flow channel) between 20 μm and 40 μm. The thickness of the layer (SU-8) on the surface electrode was measured by the stylus (with 3×10<sup>-5</sup> N) of the contact profilometer. The photoresist was baked at the hotplate.

The photomask C was mounted on the surface of SU-8, and the photoresist was exposed to the UV light through the photomask in the mask aligner. The photoresist was baked at the hotplate. The photoresist was developed with SU-8 Developer. The surface with the micro pattern was rinsed with IPA, and with the pure water. The photoresist was baked at the hotplate.

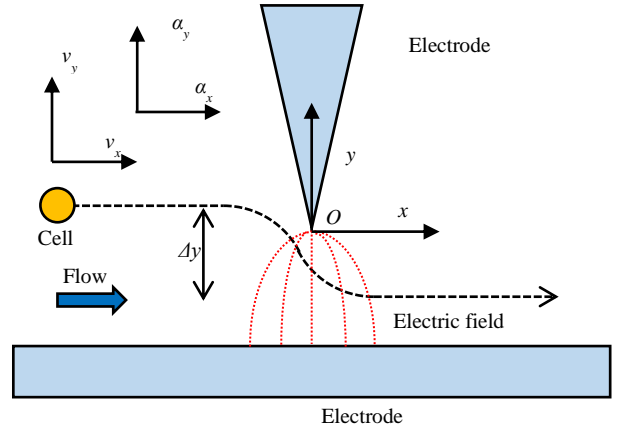


Fig. 1. Two-dimensional movement of cell flowing near tip of electrode: position  $(x, y)$ , velocity  $(v_x, v_y)$ , and acceleration  $(\alpha_x, \alpha_y)$  of cell.

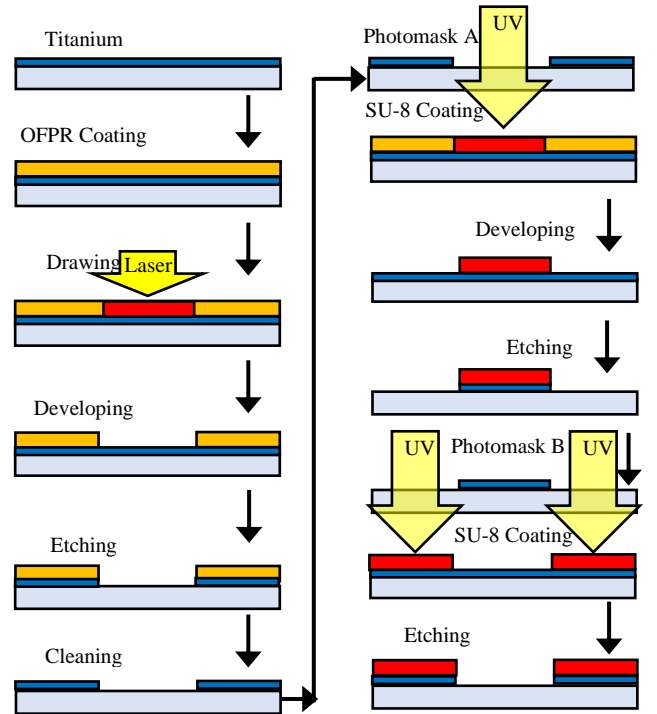


Fig. 2. Photolithography process for surface electrodes.

#### G. Upper Plate of Flow Channel

Polydimethylsiloxane (PDMS) was poured into the mold of poly-methyl-methacrylate with the curing agent. The volume ratio of PDMS to curing agent is ten to one. After degassing, PDMS was baked at 353 K for two hours in the oven. The upper plate has holes with the diameter of 5 mm for the inlet and the outlet of the suspension. The upper plate was exposed to the oxygen gas in the reactive ion etching system (FA-1), and coated with Aminopropyltriethoxysilane. After ten minutes, the upper plate was adhered on the lower plate under the pressure of 0.5 N/m<sup>2</sup> by sandwiching between plates of polymethylmethacrylate. The plates were baked in the oven at 353 K for ten minutes. A rectangular parallelepiped channel of 18 mm length × 0.5 mm width × 35 μm height is formed between upper and lower plates. The

flow channel is placed on the stage of the inverted phase-contrast microscope.

#### H. Electric Stimulation

The electric stimulation of the alternating square wave ( $0.25 \mu\text{s} < \text{period} < 10 \mu\text{s}$  ( $0.1 \text{ MHz} < \text{frequency} (f) < 4 \text{ MHz}$ ); amplitude of  $\pm 5 \text{ V}$ ,  $\pm 10 \text{ V}$ , or  $\pm 15 \text{ V}$ ) was generated with an electric stimulator. The stimulator was connected to the titanium film electrode, and the electric stimulation was applied to the medium flow. An electric resistance ( $R$ ) of  $2 \text{ k}\Omega$  is serially inserted between the electrode and the stimulator. The electric signal between the terminals of the resistance ( $V$ ) was monitored to measure the electric current by an oscilloscope during the electric stimulation applied between the titanium surface electrodes.

#### I. Cell

C2C12 (mouse myoblast cell line originated with cross-striated muscle of C3H mouse) was used in the test. D-MEM (Dulbecco's Modified Eagle Medium) containing 10% FBS (Fetal Bovine Serum) and 1% penicillin/ streptomycin was used for the medium.

Before the flow test, the inner surface of the flow channel was hydrophilized by the oxygen plasma ashing. The bovine serum albumin solution was pre-filled in the flow channel, and incubated for thirty minutes at  $310 \text{ K}$  in the incubator.

Before the flow test, cells were exfoliated from the plate of the culture dish with trypsin including EDTA (ethylenediaminetetraacetic acid), and suspended in the medium. The suspension of cells was poured at the inlet of the flow channel. The flow was made by the pressure difference between the inlet and the outlet, which was kept by the gravitational level of the medium ( $< 5 \text{ mm}$ ).

Each cell passing between the electrodes was observed by the inverted phase-contrast microscope, and recorded by the video camera, which is set at the eyepiece of the microscope. The contour of each cell was traced, and the projected two-dimensional area ( $S$ ) at the image of each cell was calculated. The equivalent radius ( $r$ ) was calculated by (1).

$$S = \pi r^2 \quad (1)$$

To trace the movement of the cell, the coordinates are defined as that in Fig. 1. The main flow direction of the medium is defined as  $x$ . The direction perpendicular to  $x$  is defined as  $y$ : the direction from the reference electrode to the tip of the triangular electrode. The origin is adjusted at the tip of the triangular electrode. Both the position ( $x_0, y_0$ ) and the velocity ( $v_0$ ) of each cell were measured at  $x = -0.4 \text{ mm}$  (upstream from the tip of the electrode) as the initial value. The shifted distance ( $\Delta y$ ) was defined as the difference between the maximum value of  $y$  coordinate and minimum value of  $y$  coordinate according to the stream line of each cell in the range of  $x$  between  $-0.4 \text{ mm}$  and  $0.4 \text{ mm}$ . The components ( $v_x$ , and  $v_y$ ) of velocity were calculated at the position tracings of each cell. The components ( $\alpha_x$ , and  $\alpha_y$ ) of the acceleration of the velocity were calculated at the velocity tracings of each cell. The maximum absolute value of the acceleration ( $\alpha_{y\text{max}}$ ) was defined according to the stream line of each cell in the range of  $x$  between  $-0.4 \text{ mm}$  and  $0.4 \text{ mm}$  (Fig. 8).

### III. RESULTS

The microscopic image (Fig. 3) exemplifies a cell flowing near the tip of the triangular electrode. The movie showed the sifted movement of the flowing cell passing adjacent to the tip of the electrode by dielectrophoresis.

Tracings of 20 cells under the electric stimulation is exemplified in Fig. 4: the period of  $0.3 \mu\text{s}$ , the amplitude of  $\pm 15 \text{ V}$ . Every cell shows the shifted movement perpendicular to the flow direction near the tip (origin) of the triangular electrode.

Fig. 5 shows the shifted distance ( $\Delta y$ ) in relation to the amplitude of the rectangular alternating voltage ( $E$ ) at the frequency ( $f$ ) of  $3 \text{ MHz}$ . The mark shows the mean value of  $\Delta y$ , and the bar shows the standard deviation. The shifted distance increases with the increase of the amplitude of the voltage. With the amplitude of  $\pm 15 \text{ V}$ , the electric current ( $I$ ) was  $\pm 7.5 \text{ mA}$ . To get enough shift movement, the amplitude of  $\pm 15 \text{ V}$  has been selected in Figs. 6-8.

The relationship between the shifted distance ( $\Delta y$ ) and the frequency ( $f$ ) of cyclic rectangular alternating electric stimulation at the amplitude of  $\pm 15 \text{ V}$  is displayed in Fig. 6. The shifted distance increases with the frequency of the cyclic stimulation. To get enough shift movement, the frequency higher than  $3 \text{ MHz}$  has been selected in Fig. 7 and Fig. 8.

Fig. 7 shows the tracings of the acceleration ( $\alpha_y$ ) of 20 cells. The period of the rectangular cyclic wave is  $0.25 \mu\text{s}$ . Each cell is accelerated to the apart direction ( $-y$  direction perpendicular to the flow) from the tip of the triangular electrode before passing through the tip of the electrode, and decelerated after passing through the tip of the electrode ( $+y$  direction).

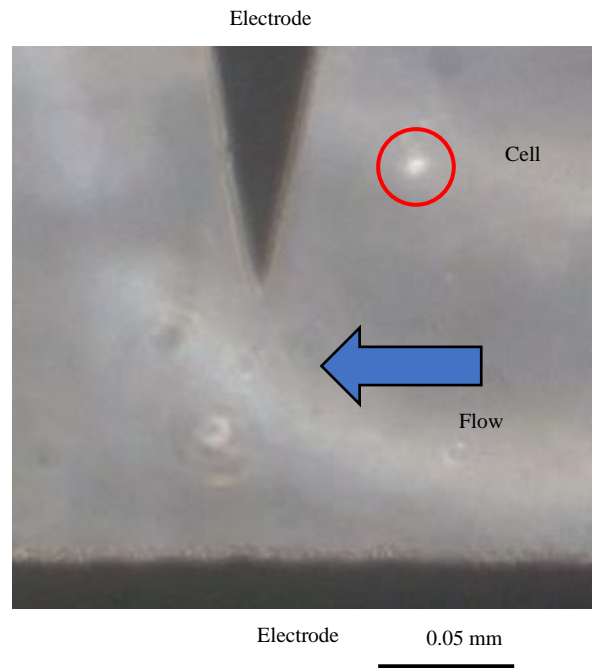


Fig. 3. Cell (red circle) is passing adjacent to tip of electrode.

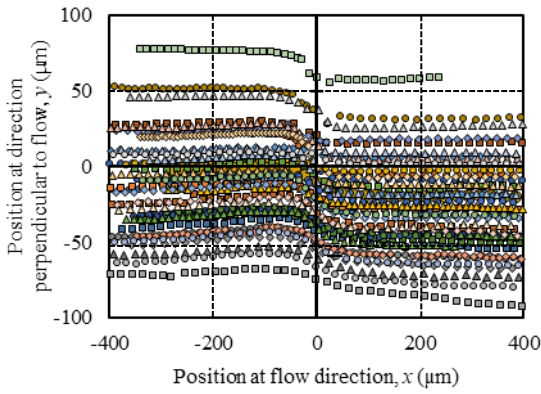


Fig. 4. Tracings of movement of 20 cells ( $\mu\text{m}$ ): frequency of 3 MHz, amplitude of  $\pm 15$  V.

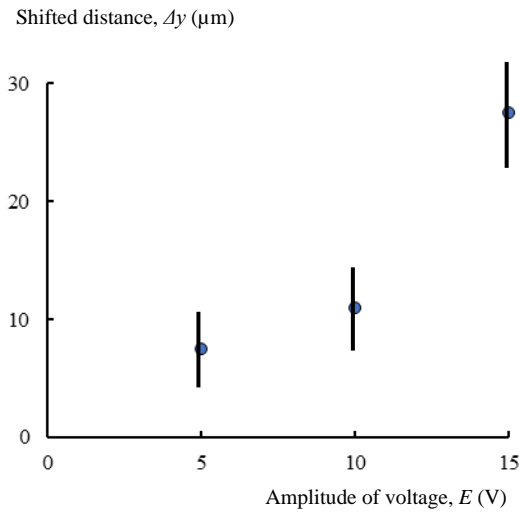


Fig. 5. Relationship between shifted distance  $\Delta y$  ( $\mu\text{m}$ ) and amplitude of voltage  $E$  (V): mean (circle)  $\pm$  standard deviation (bar), number of sample  $n = 4$ .

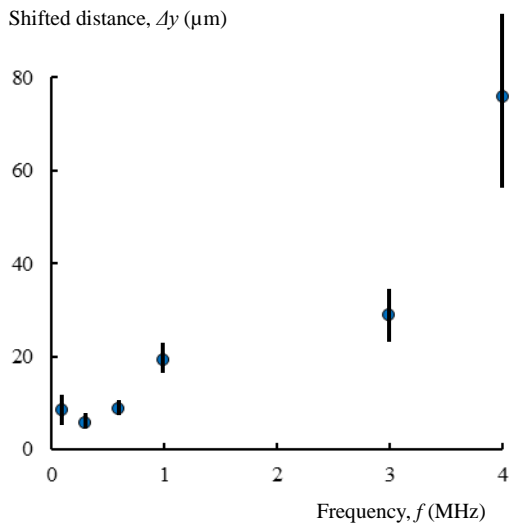


Fig. 6. Relationship between shifted distance  $\Delta y$  ( $\mu\text{m}$ ) and frequency  $f$  (MHz) of electric stimulation: mean (mark)  $\pm$  standard deviation (bar): number of sample  $n = 4$ .

Fig. 8 displays the relationship among parameters by three-dimensional graph: the maximum acceleration ( $\alpha_{y\text{max}}$ ), the radius ( $r$ ), and the initial position ( $-90 \mu\text{m} < y_0 < 60 \mu\text{m}$ ). The period of the rectangular cyclic wave is  $0.3 \mu\text{s}$ . The absolute value of the maximum amplitude of the acceleration ( $\alpha_{y\text{max}}$ ) of the velocity of each cell during passing over the tip of the electrode is displayed in Fig. 8. The absolute value of the maximum amplitude of the acceleration ( $\alpha_{y\text{max}}$ ) is high, when the cell flowing along the streamline “ $y_0 = 0$ ” through the tip of the electrode. The absolute value of the maximum amplitude of the acceleration ( $\alpha_{y\text{max}} < 13 \text{ mm/s}^2$ ) by the electric field, which is perpendicular to the flow direction, increases with the radius of the cell ( $r < 11 \mu\text{m}$ ).

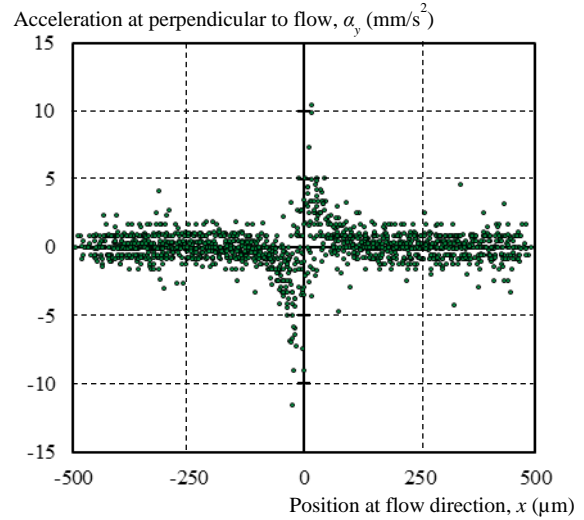


Fig. 7. Acceleration  $\alpha_y$  ( $\text{mm/s}^2$ ) tracings of 20 cells: frequency  $f$  of 4 MHz, amplitude  $E$  of  $\pm 15$  V.

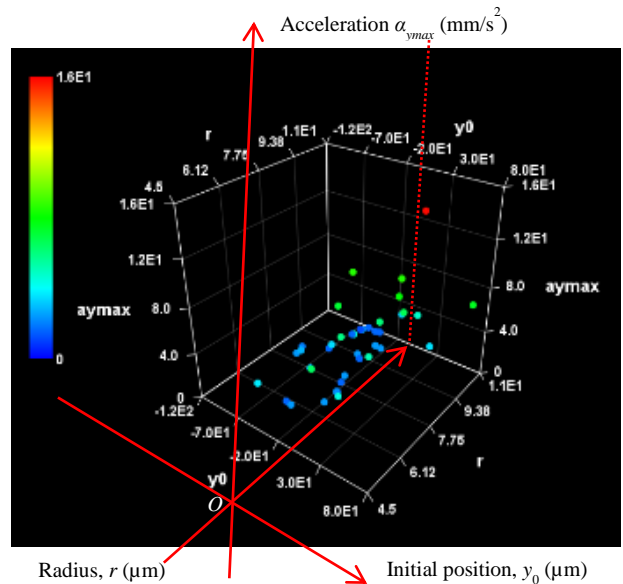


Fig. 8. Relationship among maximum acceleration  $\alpha_{y\text{max}}$  ( $\text{mm/s}^2$ ), radius  $r$  ( $\mu\text{m}$ ), and initial position  $y_0$  ( $\mu\text{m}$ ): frequency of 3 MHz, amplitude of  $\pm 15$  V.

#### IV. DISCUSSION

To find optimum design of the microdevice for the experiment of dielectrophoresis, variations were made at several parameters in previous studies: the shape of electrodes, and the waveform of the electric stimulation (the amplitude, and the frequency) [20]. At 4 MHz, the dielectrophoretic movement of each cell was not able to be detected by alternating current of the sine wave. With the alternating current of the square wave at 4 MHz, on the other hand, the dielectrophoretic movement of each cell has been detected.

The rectangular fluctuating voltage between electrodes [21] with the amplitude of  $\pm 15$  V (the amplitude of electric current of  $\pm 7.5$  mA) made the enlarged lateral shift of the flowing cell (Fig. 5). The amplitude of the electric stimulation has been limited within the threshold value to prevent electrolysis [22] in the present study.

Dielectrophoresis was applied to the cell sorting system as the minimally invasive method in a lot of previous studies [23]. Before passing through the non-uniform electric field in the flow channel, both the initial position and the velocity [24] should be controlled.

In the present study, the dielectrophoretic movement of the cell has been tried to be observed by the optical microscope. In the present study, the couple of electrodes arrangement with the shorter distance each other has not been designed, because the electrodes are not optically transparent to observe the movement near the electrode optically. The shift depends on the passing route position of the cell relative to the position of the tip of the electrode. The dielectrophoretic effect is highest adjacent to the tip of the electrode [25].

Fig. 4 shows the two-dimensional movement of each cell in the  $x$ - $y$  plane from the microscopic video image. The real movement of each cell is three-dimensional. The movement of the perpendicular direction to  $x$ - $y$  plane is very small, because the height (35  $\mu\text{m}$ ) of the flow channel is small compared with the width (0.5 mm) of the flow channel in the present experiment. The height is also close to the diameter ( $d$ ) of the cell ( $10 \mu\text{m} < d < 25 \mu\text{m}$ ) used in the present study. The position of the streamline of the target cell was tried to be controlled before passing through the electric field area in the previous study [26].

The movement of cells between surface electrodes depends on the topography of surface electrodes (the angle of the tip) [27], which relates to non-uniformity of the electric field. The higher slope of the electric field with non-uniformity is necessary to enlarge the movement of each cell around the electrode.

In principle, dielectrophoretic effect increases with the diameter of the particle. In the present experiment, it is confirmed that the acceleration of the cell along the electric field (perpendicular to the flow direction) increases with the radius of the cell (Fig. 8). In the present microfluidic channel, 10  $\text{mm/s}^2$  increase of the lateral acceleration has been generated per 5  $\mu\text{m}$  increase of the radius of the cell.

The shifted distance of each cell is rather small at the single pair of electrodes. If the lateral shift movement of the cell adjacent to the tip of the electrode is enlarged at the downstream by the inertial movement, the method can be applied to the cell sorting. In the present device, the lateral

shift of 70  $\mu\text{m}$  has been realized [28]. The lateral shift can be amplified by accumulation with the multi-electrodes system on the flow channel [29]. The relationship between the streamline of the cell and the position of the side wall of the flow channel should be considered for the continuous movement of the cell downstream.

Polydimethylsiloxane is available to make the micro surface topography [30] for experimental devices on biological cells. Biological cells are sensitive to the micro surface topography on the scaffold [31]. The micro grooves, on the other hand, were used for trapping of flowing cells in the previous study [32]. The system had capability to separate the malnourished cell.

In the previous studies, dielectrophoresis was tried to be applied to the biological cell manipulation technology [33]. The present study shows that the dielectrophoretic movement through the micro channel with asymmetric surface electrodes fabricated by the photolithography technique is effective to sort flowing cells. The cell sorting technology would be applied to tissue engineering [34] (e.g., the bio-actuator made from myoblasts [35]). The cell sorting can be applied to select targeted cells to improve the efficiency to make the tissue. The cell sorting technology would also be applied to diagnostics in medicine: detection of cancer cells [36].

#### V. CONCLUSION

The flow channel with asymmetric electrodes has been designed by photolithography technique to detect dielectrophoresis. The micro system has realized that the absolute value of the amplitude of the acceleration by the electric field, which is perpendicular to the flow direction, increases with the radius of the cell.

#### ACKNOWLEDGMENT

The authors thank to Mr. Daisuke Hasegawa and to Mr. Ryota Matsuzawa for their assistance of the experiment.

#### REFERENCES

- [1] S. Hashimoto, "Oblique micro grooves on bottom wall of flow channel to sort cells," Proc. ASME 2020 Fluids Engineering Division Summer Meeting, FEDSM2020-20096, 2020, pp. 1–6.
- [2] A. Tabll, and H. Ismail, "Chapter 7: The use of flow cytometric DNA ploidy analysis of liver biopsies in liver cirrhosis and hepatocellular carcinoma," Liver Biopsy, H. Takahashi, Ed, Intech Open Limited, 2011, pp. 88–107.
- [3] S. Hashimoto, H. Sugimoto, and H. Hino, "Effect of couette type of shear stress field with axial shear slope on deformation and migration of cell: comparison between C2C12 and HUVEC," Journal of Systemics, Cybernetics and Informatics, vol. 17, no. 2, 2019, pp. 4–10.
- [4] S. M. McFaul, B. K. Lin, and H. Ma, "Cell separation based on size and deformability using microfluidic funnel ratchets," Lab on a Chip, vol. 12, 2012, pp. 2369–2376.
- [5] Y. Takahashi, S. Hashimoto, H. Hino, and T. Azuma, "Design of slit between micro cylindrical pillars for cell sorting," Journal of Systemics, Cybernetics and Informatics, vol. 14, no. 6, 2016, pp. 8–14.
- [6] S. Hashimoto, "Micro machined slit between ridge and groove in micro fluid-channel to measure floating cell deformability," Proc. ASME 2020 Fluids Engineering Division Summer Meeting, FEDSM2020-20073, 2020, pp. 1–7.
- [7] M. Heijazian, W. Li, and N. T. Nguyen, "Lab on a chip for continuous-flow magnetic cell separation," Lab on a Chip, vol. 15, no. 4, 2015, pp. 959–970.

- [8] H. Imasato, and T. Yamakawa, "Measurement of dielectrophoretic force by employing controllable gravitational force," *Journal of Electrophoresis*, vol. 52, no. 1, 2008, pp. 1–8.
- [9] A. Miyakawa, T. Ishikawa, and Y. Kawata, "The examination of basic condition of the single cell isolation with laser," *Laser Original*, vol. 39, no. 2, 2011, pp. 123–128.
- [10] D. R. Gossett, W. M. Weaver, A. J. Mach, S. C. Hur, H. T. K. Tse, W. Lee, H. Amini, and D. DiCarlo, "Label-free cell separation and sorting in microfluidic systems," *Analytical and Bioanalytical Chemistry*, vol. 397, 2010, pp. 3249–3267.
- [11] B. Yafouz, N. A. Kadri, and F. Ibrahim, "Dielectrophoretic manipulation and separation of microparticles using microarray dot electrodes," *Sensors*, vol. 14, no. 4, 2014, pp. 6356–6369.
- [12] P. R. C. Gascoyne, X. B. Wang, Y. Huang, and F. F. Becker, "Dielectrophoretic separation of cancer cells from blood," *IEEE Transactions on Industry Applications*, vol. 33, no. 3, 1997, pp. 670–678.
- [13] M. D. Vahey, and J. Voldman, "An equilibrium method for continuous-flow cell sorting using dielectrophoresis," *Analytical Chemistry*, vol. 80, no. 9, 2008, pp. 3135–3143.
- [14] T. Müller, A. Pfennig, P. Klein, G. Gradl, M. Jäger, and T. Schnelle, "The potential of dielectrophoresis for single-cell experiments," *IEEE Engineering in Medicine and Biology Magazine*, no. 11/12, 2003, pp. 51–61.
- [15] X. Xuan, B. Xu, and D. Li, "Accelerated particle electrophoretic motion and separation in converging-diverging microchannels," *Analytical Chemistry*, vol. 77, no. 14, 2005, pp. 4323–4328.
- [16] H. Imasato, and T. Yamakawa, "Measurement of dielectrophoretic force by employing controllable gravitational force," *Journal of Electrophoresis*, vol. 52, no. 1, 2008, pp. 1–8.
- [17] Y. Kang, D-D. Li, S. A. Kalams, and J. E. Eid, "DC-dielectrophoretic separation of biological cells by size," *Biomedical Microdevices*, vol. 10, no. 2, 2008, pp. 243–249.
- [18] H. C. Shim, Y. K. Kwak, C. S. Han, and S. Kim, "Effect of a square wave on an assembly of multi-walled carbon nanotubes using AC dielectrophoresis," *Physica E*, vol. 41, 2009, pp. 1137–1142.
- [19] B. H. Jo, L. M. Van Lerberghe, K. M. Motsegood, and D. J. Beebe, "Three-Dimensional Micro-Channel Fabrication in Polydimethylsiloxane (PDMS) Elastomer," *Journal of Microelectromechanical Systems*, vol. 9, no. 1, 2000, pp. 76–81.
- [20] Y. Takahashi, S. Hashimoto, R. Yamauchi, H. Hino, and T. Yasuda, "Myoblast behavior around surface electrodes in flow channel," *Proc. 21st World Multi-Conference on Systemics Cybernetics and Informatics*, vol. 2, 2017, pp. 251–256.
- [21] H. Chu, I. Doh, and Y. H. Cho, "A three-dimensional (3D) particle focusing channel using the positive dielectrophoresis (pDEP) guided by a dielectric structure between two planar electrodes," *Lab on a Chip*, vol. 9, no. 5, 2009, pp. 686–691.
- [22] G. Mernier, N. Piacentini, T. Braschler, N. Demierre, and P. Renaud, "Continuous-flow electrical lysis device with integrated control by dielectrophoretic cell sorting," *Lab on a Chip*, vol. 10, no. 16, 2010, pp. 2077–2082.
- [23] K. Zhao, L. B. P. Duncker, and D. Li, "Continuous cell characterization and separation by microfluidic alternating current dielectrophoresis," *Analytical Chemistry*, vol. 91, 2019, pp. 6304–6314.
- [24] J. G. Gao, R. Riahi, M. L. Y. Sina, S. Zhang, and P. K. Wonga, "Electrokinetic focusing and separation of mammalian cells in conductive biological fluids," *Analyst*, vol. 137, no. 22, 2012, pp. 5215–5221.
- [25] Y. Wakizaka, M. Hakoda, and N. Shiragami, "Effect of electrode geometry on dielectrophoretic separation of cells," *Biochemical Engineering Journal*, vol. 20, no. 1, 2004, pp. 13–19.
- [26] X. Chen, Y. Ren, W. Liu, X. Feng, Y. Jia, Y. Tao, and H. Jiang, "A simplified microfluidic device for particle separation with two consecutive steps: induced charge electro-osmotic prefocusing and dielectrophoretic separation," *Analytical Chemistry*, vol. 89, 2017, pp. 9583–9592.
- [27] N. Demierre, T. Braschler, P. Linderholm, U. Seger, H. van Lintel, and P. Renaud, "Characterization and optimization of liquid electrodes for lateral dielectrophoresis," *Lab on a Chip*, vol. 7, no. 3, 2007, pp. 355–365.
- [28] S. Hashimoto, R. Matsuzawa, and Y. Endo, "Analysis of dielectrophoretic movement of floating myoblast near surface electrodes in flow channel," *Proc. 11th International Multi-Conference on Complexity Informatics and Cybernetics*, vol. 2, 2020, pp. 13–18.
- [29] J. Giesler, G. R. Pesch, L. Weirauch, M. P. Schmidt, J. Thöming, and M. Baune, "Polarizability-dependent sorting of microparticles using continuous-flow dielectrophoretic chromatography with a frequency modulation method," *Micromachines*, vol. 11, no. 38, 2019, pp. 1–14.
- [30] P. N. Carlsen, Ed., *Polydimethylsiloxane: Structure and Applications*, Nova Science Publishers, 2020 (S. Hashimoto, Application of polydimethylsiloxane: microstructure of functional surface for observation of biological cell behavior, pp. 29–94).
- [31] S. Hashimoto, and K. Abe, "Monitoring of orientation of cells by electric impedance: test on oriented cells using micro striped grooves pattern by photolithography," *Proc. IEEE 19th International Conference on Bioinformatics and Bioengineering (BIBE)*, 2019, pp. 557–562.
- [32] Y. Takahashi, S. Hashimoto, H. Hino, A. Mizoi, and N. Noguchi, "Micro groove for trapping of flowing cell," *Journal of Systemics Cybernetics and Informatics*, vol. 13, no. 3, 2015, pp. 1–8.
- [33] H. Shafiee, J. L. Caldwell, M. B. Sano, and R. V. Davalos, "Contactless dielectrophoresis: a new technique for cell manipulation," *Biomedical Microdevices*, vol. 11, no. 5, 2009, pp. 997–1006.
- [34] C. A. Powell, B. L. Smiley, J. Mills, and H. H. Vandenburg, "Mechanical stimulation improves tissue-engineered human skeletal muscle," *American Journal of Physiology - Cell Physiology*, vol. 283, no. 5, 2002, pp. C1557–C1565.
- [35] S. V. Anand, M. Y. Ali, and M. T. A. Saif, "Cell culture on microfabricated one-dimensional polymeric structures for bio-actuator and bio-bot applications," *Lab on a Chip*, vol. 15, no. 8, 2015, pp. 1879–1888.
- [36] J. An, J. Lee, S. H. Lee, J. Park, and B. Kim, "Separation of malignant human breast cancer epithelial cells from healthy epithelial cells using an advanced dielectrophoresis-activated cell sorter (DACS)," *Analytical and Bioanalytical Chemistry*, vol. 394, no. 3, 2009, pp. 801–809.